DEVELOPMENTS OF THE FZP BEAM PROFILE MONITOR

N. Nakamura, H. Sakai, H. Takaki, M. Fujisawa, K. Shinoe, H. Kudo, T. Tanaka
ISSP, University of Tokyo, 5-1-5 Kashiwanoha, Kashiwa, Chiba 277-8581, Japan
T. Muto, H. Hayano, KEK, 1-1 Oho, Tsukuba, Ibaraki 305-0801, Japan

Abstract

We present recent developments of the FZP (Fresnel zone plate) beam profile monitor constructed at KEK-ATF damping ring, which is a real-time and high-resolution monitor using an X-ray imaging optics based on two FZPs. The crystal monochromator and the FZP holders were newly fabricated for suppression of the beam image drift and achievement of precise beam-based alignment and an X-ray pinhole mask was additionally installed for reduction of the undesirable background component. The radiation damping time and the intrabeam scattering and emittance coupling effects were successfully measured with this monitor. Effects of aberrations due to FZP alignment errors and vibrations of the FZPs were estimated and concluded not to seriously deteriorate the spatial resolution of the monitor.

INTRODUCTION

A beam profile monitor based on two Fresnel zone plates (FZPs) has been developed at the KEK-ATF (Accelerator Test Facility) damping ring. In the monitor beamline, the synchrotron radiation from the electron beam is monochromatized by a crystal monochromator and the transverse beam image is twenty-times magnified by the two zone plates (CZP and MZP) and detected on the X-ray CCD camera. This monitor can take real-time images of the electron beam and measure the beam profiles with a high spatial resolution of less than 1 μm in the standard deviation of the Gaussian distribution. Clear electron-beam images with the vertical beam sizes less than 10 μm were obtained in the early measurements [1]. Recently some of the optical elements were improved and beam behaviours due to the radiation damping, intrabeam scattering and emittance coupling effects were observed with this monitor. In addition, aberrations due to FZP alignment errors were studied and FZP vibrations were measured in order to estimate their effects on the spatial resolution of the monitor. In this paper, we will present the recent progress of the beam profile monitor.

IMPROVEMENT

Recent improvement of the FZP beam profile monitor is described here. The system layout is shown in Fig. 1.

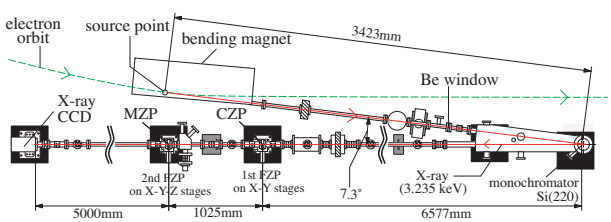

Figure 1. Layout of the FZP beam profile monitor

Monochromator

The vertical position of the beam image on the CCD had largely drifted after operation of the stepping motor adjusting the angle of the silicon crystal to the vertical axis, because the support of the silicon crystal in the previous monochromator was deformed by the heat from the stepping motor. The new monochromator was made in order to suppress the angle drift of the crystal. In the new monochromator, the stepping motor was thermally isolated from the main part of the monochromator by ceramic insulators and thermally stabilized by copper lines cooled by the water. After this improvement, the drift was reduced by a factor of about 100.

FZP holders

New FZP holders were designed and fabricated so that the FZPs could be removed up from the optical path in the vacuum when necessary. The removed FZPs are protected from the air pressure during leaks in maintenance and repair of the monitor beamline or installation of new beamline components. They have never been damaged by the air pressure since installation of the new holders. Furthermore the new holders allowed us to establish a more precise beam-based alignment scheme using only the X-ray CCD camera. In the previous alignment, three fluorescence screens sensitive to X-rays installed just after the monochromator, just before the CZP and between the CZP and the MZP were used, because the X-ray beam intercepted by the FZPs fixed in the previous holders could not be detected with the X-ray CCD. In the new alignment, first the center position of the X-ray beam reflected at the silicon crystal (corresponding to the position of the optical axis) is measured with the X-ray CCD and then, after inserting the CZP on the optical path, the CZP position is adjusted to set the center position of the transmitted X-rays through the CZP to the position of the optical axis. Finally the MZP position is adjusted to set the beam image position to the position of the optical axis after inserting the MZP on the optical path. The minimum position error is about one pixel of the CCD (24 μm) for the CZP and 1/200 (the reciprocal of the MZP magnification) of one pixel for the MZP. The FZP tilt angle to the optical axis is decided mainly by the machining accuracy and it is estimated to be less than 0.5°.

X-ray pinhole mask

The transmitted X-rays through the MZP, one of the background components, appear on the X-ray CCD as a square of about 3 mm x 3 mm, reflecting the MZP structure. An X-ray mask system with a pinhole was installed near the focus point of the CZP to reduce the

background component of the transmitted X-rays. The X-ray mask is made of stainless steel and can be moved in the horizontal and vertical directions. Figure 2 shows the CCD images before and after insertion of the X-ray mask with the pinhole diameter of 300 μm. The area of the background component was reduced by a factor of 100 with this X-ray mask.

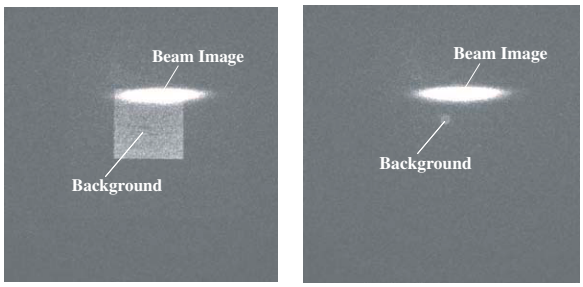

(a) (b)

Figure 2: CCD images (a) before and (b) after insertion of the X-ray mask with the pinhole diameter of 300 μm.

MEASUREMENT

Radiation damping time

The radiation damping time is an important parameter especially for the damping ring. It was obtained by measuring time dependence of the vertical beam size after injection from the injector linac to the damping ring. The X-ray CCD camera and the X-ray shutter were synchronized with the injection trigger signals in this measurement. Figure 3 shows the measured time dependence of the vertical beam size. The vertical beam size decreased with time after injection and then reached the equilibrium state, as shown in Fig. 3. By fitting the measured data (solid squares) to an exponential curve, the radiation damping time was obtained to be about 25 ms. This is in good agreement with the design value.

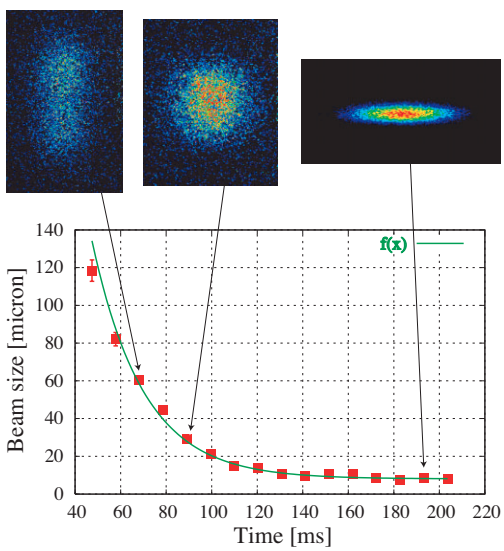

Figure 3. Time dependence of the vertical beam size after injection from the injector linac to the damping ring. Three beam images at three different times are also shown.

Current and coupling dependences

The KEK-ATF damping ring can be affected by intrabeam scattering because of the extremely low emittance of about 1 nmrad. Figure 4 shows bunch current dependences of the horizontal and vertical beam sizes measured by the beam profile monitor. The horizontal beam size significantly increased with bunch current because the momentum spread increased due to intrabeam scattering and the SR source point had a considerable horizontal momentum dispersion. The coupling dependences were also measured by changing currents of the skew-quadrupole coils wound on two kinds of sextupole magnets, "SD" and "SF". As shown in Fig. 4, the vertical beam size increased with the emittance coupling, while the horizontal one decreased. The emittance coupling effect was clearly found in this experiment.

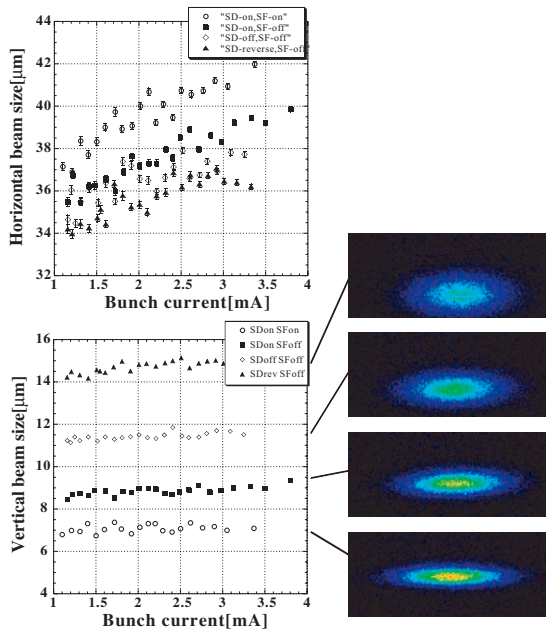

Figure 4. Current and coupling dependences of beam size measured by the beam profile monitor. Four beam images corresponding to four coupling states are also shown.

ABERRATION AND VIBRATION EFFECTS

Aberrations due to alignment errors

Aberrations due to the FZP alignment errors are estimated here. The imaging optics of the beam profile monitor is schematically shown in Fig. 5. Let ψ, a and b be the tilt angle of the FZP and the distances from the source point to the FZP center and from the FZP center to the focus point. The optical path difference between X-rays incident on the center and the outermost part of the FZP is calculated and apprximated under the assumption of $r_N << a$, b and $\psi << 1$, where r_N is the FZP radius. According to the Rayleigh's criterion, the tilt angle for which the aberrations are negligible is obtained from the following inequality:

$$\left| -\frac{1}{2}\left(\frac{1}{a}+\frac{1}{b}\right) r_N{}^2\psi^2 \pm \frac{1}{2}\left(-\frac{1}{a^2}+\frac{1}{b^2}\right) r_N{}^3\psi - \frac{1}{8}\left(\frac{1}{a^3}+\frac{1}{b^3}\right) r_N{}^4 \right| < \frac{\lambda}{4} \quad (1)$$

Here λ is the wavelength of the X-ray and 0.383 nm for our system. The first term in the left side of (1) is both astigmatism and field curvature and the second and third terms are the coma and axial spherical aberrations. The plus and minus signs of the second term correspond to X-rays incident on the upper and the lower part of the FZP. The allowable tilt angle for the good-focusing condition is less than about 0.5° for the CZP (a=10m, b=1m and r_N=1.5mm) and 3.4° for the MZP (a=0.025m, b=5m and r_N=37.3μm). The tilt of the CZP causes larger aberrations by a factor of about seven than that of the MZP. This result is consistent with a ray-tracing analysis, where the image size of a point source caused by the aberrations is less than the spatial resolution of the imaging optics (0.6 μm) within the allowable tilt angles of the CZP and the MZP [2]. The aberrations due to the tilt angle of 0.5° (CZP) and 3.4° (MZP) almost correspond to those due to the position errors of 87 mm (CZP) and 1.5 mm (MZP). The present alignment precision described in the previous section satisfies the good-focusing condition required for the tilt angles and the position errors of the FZPs. Aberration calculation based on the wave optics is also in progress and will be described elsewhere [3].

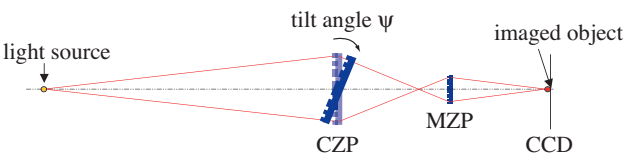

Figure 5: Schematic view of the imaging optics based on the two FZPs in the beam profile monitor.

FZP vibrations

Vibrations of the FZPs can deteriorate the spatial resolution of the monitor. The image sizes of a point source on the CCD caused by the CZP and MZP vibrations with an r.m.s. displacement of Δy are $M_{MZP}(1+M_{CZP})\Delta y$ and $M_{MZP}\Delta y$, respectively. Here M_{CZP} and M_{MZP} are magnifications of the CZP and the MZP. By dividing the image sizes on the CCD by the optics magnification of $M = M_{MZP} \times M_{CZP}$, the normalized image sizes to the light source scale are obtained to be $(1+1/M_{CZP})\Delta y$ and $(1/M_{CZP})\Delta y$, respectively. For our monitor (M_{MZP}=0.1 and M_{MZP}=200), they are $11\Delta y$ and $10\Delta y$. Vibrations of the optical elements were measured at frequencies below 100 Hz with a compact seismometer (VSE-15D from Tokyo Sokushin Corporation). Figure 6 shows the measurement results of vertical vibrations on the two FZP holders. The cumulative displacement at each frequency is defined by square root of the displacement power spectrum reversely integrated from the 100 Hz to the frequency. The cumulative displacements at 1 Hz are less than 0.1 μm for both CZP and MZP and hence the normalized vertical image sizes of a point source caused by the vibrations are estimated to be about 1 μm or less for the usual CCD exposure time of much shorter than 1 s (20 ms at minimum), which nearly equals the spatial resolution of the monitor. For the two FZPs, the measured horizontal cumulative displacements at 1 Hz are slightly larger than the vertical ones. Since the horizontal beam size in the damping ring is larger by about several times than the vertical one, the effect of the horizontal vibrations is less serious.

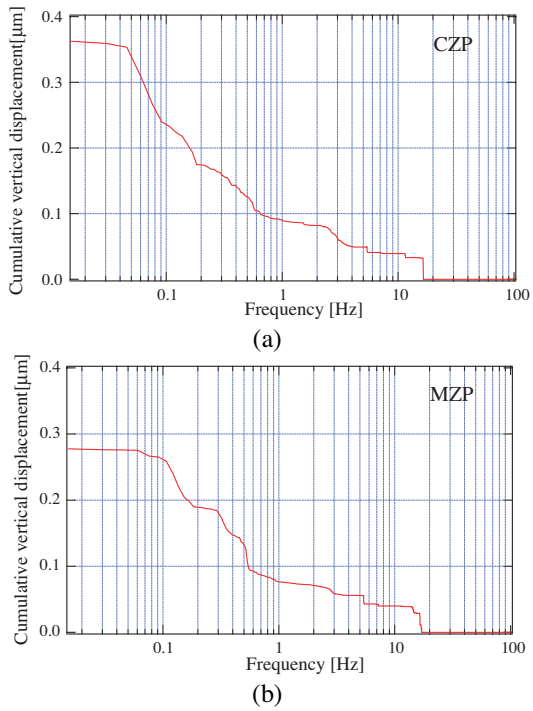

Figure 6: Cumulative vertical displacement on (a) the CZP and (b) the MZP holders.

SUMMARY

The angle drift of the silicon crystal was drastically suppressed by the new monochromator and the FZPs became movable in the vacuum by the new FZP holders, which also helped to establish a more precise beam-based alignment scheme. The background of X-rays passing through the MZP was greatly reduced by installation of the X-ray pinhole mask. With the beam profile monitor, the radiation damping time was experimentally obtained and the intrabeam scattering and emittance coupling effects were clearly observed. Aberrations due to FZP alignment errors were studied and vibrations on the FZP holders were measured. Their effects on the spatial resolution of the monitor were not serious for measuring the electron beam sizes in the KEK-ATF damping ring.

REFERENCES

[1] K. Iida et al., Nucl. Instrum. and Meth. A506 (2003) 41-49; N. Nakamura et al., Proc. of PAC 03, Portland, 2003, p.530.
[2] M. Fujisawa et al., to be submitted to Journal of Synchrotron Radiation.
[3] T. Muto, private communication.